ANFIS Granger Causality for Estimating Effective Brain Connectivity and Mutual Information for Connectivity Type Determination Using MEG and EEG Data: Application to Epilepsy

Erfan Vajdi [iD], Morteza Fattahi [iD], Hamid Soltanian-Zadeh* [iD]

School of Electrical and Computer Engineering, University of Tehran, Tehran, Iran.

ABSTRACT: In the scientific community, it is well established that the brain is linked to neural disorders such as epilepsy, Alzheimer's, and depression, all of which can affect neural connectivity. These conditions can disrupt communication between different brain regions. To assess these changes, neuroscientists measure neural signals like EEG and MEG and analyze brain connectivity through scalp recordings. Various methods have been developed to evaluate intra-brain connectivity, including classical techniques such as Granger causality (GC), Mutual Information (MI), Directed Transfer Function (DTF), and Dynamic Causal Modeling (DCM). Recently, there has been increasing interest in applying neural networks as a modern approach across various fields. However, many existing methods suffer from low precision. This paper proposes the Adaptive Neuro-Fuzzy Inference System Granger Causality (ANFISGC) as a solution for measuring effective connectivity using EEG and MEG data. Our approach integrates symplectic geometry, ANFIS regression, and Granger causality, allowing for the detection of both linear and nonlinear causal information flow. This multivariate method can also differentiate between direct and indirect connectivity, enhancing its significance. Additionally, we utilized Mutual Information (MI) to evaluate the relationship between two variables, offering insights into the linearity or nonlinearity of connectivity. This measurement provides a further understanding of brain functionality. To assess the effectiveness of our approach, we conducted tests using simulated data and data from five epilepsy patients. The results show that measurements based on MEG data align well with clinical findings, while incorporating EEG data alongside MEG (in a multimodal approach) does not improve the results.

1- Introduction

Many brain disorders, including Alzheimer's and schizophrenia, are recognized as complex diseases. The interactions within the brain can be effectively modeled as a complex network, enhancing our understanding of information flow and functionality. Analyzing this brain network is essential for gaining insights into these disorders. Recent advancements in neuroimaging provide valuable experimental data for constructing comprehensive brain networks, uncovering topological features associated with these conditions [1]. Studying brain connectivity to map functional regions is crucial in neuroscience. Techniques such as EEG and MEG help identify connectivity between different brain regions. Granger causality is an important method for investigating effective connectivity and causal relationships within the brain [2]. The concept of causality was first introduced by Wiener, who proposed that if past information from signal X improves the prediction of signal Y, then X

exerts a causal influence on Y. Granger later reformulated this definition using linear VAR modeling. However, this linear approach poses challenges for studying the brain, which operates as a nonlinear dynamic system, making Linear Granger causality inadequate for such contexts. To address this limitation, various methods, including Kernel Granger causality (KGC) and Nonlinear Granger causality (NLGC), have been developed to explore causality in nonlinear systems [3]. The use of artificial neural networks to compute effective connectivity has garnered significant interest in recent years. In 2019, a study utilized a Multi-Layer Perceptron (MLP) network to measure nonlinear Granger causality in patients with autism, effectively distinguishing between the linear and nonlinear components of connectivity [4]. In the same year, a method for estimating effective connectivity in epilepsy patients was developed using a recurrent neural network (RNN). This approach, known as NGUEW, employed an optimization technique to identify the optimal time lag for predicting the target time series, resulting in a self-organized network structure. The study also proposed using the intensity

*Corresponding author's email: hszadeh@ut.ac.ir

31

of causality as a means to analyze effective connectivity [5]. In 2021, a 3D convolutional neural network (CNN) was used to differentiate individuals with Major Depressive Disorder (MDD) from healthy individuals. The aim was to accurately identify MDD patients by analyzing their effective connectivity patterns [6].

Recent advancements in artificial intelligence through deep learning techniques have the potential to significantly assist psychologists in diagnosing mental disorders more efficiently. One such disorder is Myotonic Muscular Dystrophy (MMD), which poses diagnostic challenges due to its ambiguous symptoms. EEG is a valuable tool for studying brain diseases, including MMD, because of its high temporal resolution and noninvasive nature. A 2021 study proposed a deep learning framework that utilized EEG data for the automatic classification of MMD patients versus healthy individuals. This framework extracted relationships between different brain channels using methods such as Generalized Partial Directed Coherence (GPDC) and Direct Directed Transfer Function (dDTF) analysis. By integrating these connectivity methods across eight frequency bands, images were generated for each individual. These EEG-derived images were then analyzed and classified using five different deep-learning architectures [7]. However, in this study, we take a different approach by applying Granger causality analysis using artificial neural networks to epileptic data. The most common method for training neural networks is gradient descent, a calculus-based technique that iteratively computes local minima of the error surface. However, this method has significant drawbacks, including the risk of not finding the global minimum, challenges in selecting an appropriate learning rate, and difficulties in minimizing highly non-convex error functions. An alternative approach to enhance the performance of deep neural networks involves creating hybrid models that incorporate fuzzy systems. Additionally, various issues can arise from low sample sizes, noisy or heterogeneous data, and severe class imbalance. To tackle these challenges specific to deep learning, multiple strategies have been proposed [8]. In a 2019 study, a deep fuzzy structure was employed to model the multivariate autoregressive framework used in Granger causality, a fundamental method for calculating effective connectivity in the brain. The proposed model leverages a hierarchical stacked architecture, with first-order TSK fuzzy rules serving as the core components of the network [9]. In 2019, researchers proposed a new model for controlling the depth of anesthesia (DOA) that moves beyond the conventional use of the Bispectral Index (BIS) signal. This innovative strategy for estimating DOA utilizes a feedforward neural network combined with an adaptive neuro-fuzzy inference model [10].

This paper presents ANFISGC, a proposed method from [11] for deriving Granger causality using the Adaptive Neuro-Fuzzy Inference System (ANFIS), a neural network predictor designed to assess conditional effective connectivity. This approach effectively identifies both linear and nonlinear relationships. A previous study [12] demonstrated that ANFISGC outperforms SMN as a causality inference

method for analyzing nonlinear, chaotic, and non-stationary datasets. To our knowledge, no study has been conducted on multimodal data for the effective connectivity of epilepsy patients. In this study, in addition to using ANFISGC, we combine EEG and MEG data to investigate whether using multimodal data (MEEG) helps improve the results. The extracted connectivities provide valuable insights into dynamic systems, such as brain networks. Our study aims to determine whether brain interactions arise from linear information flow or nonlinear processes, utilizing mutual information as a key tool.

An article [13] investigated the use of mutual information to explore corticomuscular interactions with both univariate and bivariate surrogate data, validating the approach using simulated datasets. In our study, we adopted a two-phase approach. First, we determined the conditional effective connectivities. Next, we assessed the linearity of these connections using mutual information. Section 2 details the ANFIS method, preprocessing steps, and the concept of mutual information. We also provide information about the simulated datasets and the real MEG and EEG data utilized in our analysis. These datasets were evaluated using the ANFISGC method. In the final section, we present the results from applying ANFISGC to both the simulated and original data.

2- Materials and Methods

This section offers an overview of the theory behind ANFIS, time window estimation based on symplectic geometry, Granger causality, and mutual information. Following this, we discuss how these three tools can be integrated for effective connectivity estimation, while also employing mutual information to assess linearity

2- 1- Adaptive Neuro-Fuzzy Inference System

Fuzzy logic (FL) is widely used in various modeling systems due to its effectiveness in handling imprecise and inexact information. FL translates human reasoning and concept formation into fuzzy rules. However, it faces challenges in selecting appropriate membership functions regarding both type and quantity, as well as determining suitable scaling factors for the fuzzification and defuzzification stages. To overcome these limitations, the Adaptive Neuro-Fuzzy Inference System (ANFIS) integrates the advantages of Artificial Neural Networks (ANN) to dynamically adjust the number of membership functions and their associated parameters [12].

In 1993, Jang introduced the ANFIS technique as a solution for complex and nonlinear problems. This study utilizes the ANFIS method, which integrates a fuzzy inference system within adaptive neural network structures. The adaptive system maps input data to output by leveraging human knowledge and training algorithms. These algorithms utilize predetermined input-output data and a gradient descent approach to fine-tune the premise parameters that define membership functions (MFs). Additionally, the least-squares method is employed to identify the consequent parameters

of the output equation. ANFIS is widely applied in various fields, including modeling nonlinear functions and predicting chaotic time series. It consists of five layers: the first generates membership functions, while the remaining layers perform multiplication, normalization, linear regression, and summation [14].

2- 2- Model Order Based on Embedding Dimension

To simplify computation, our focus is on a limited number of variables (system order p) that can effectively describe the entire system (brain). We have a time series $(X1,...,Xn)$, and we can reconstruct time-delay vectors (time window) as $(X_n, X_{n-\tau}, X_{n-2\tau},...,X_{n-(d-1)\tau})$ [15]. The projection of the original system into this lower-dimensional space is defined by choosing d=p. Nonlinear time series analysis serves as an effective technique for extracting insights from nonlinear dynamical systems.

A new method is proposed for determining the appropriate embedding dimension in nonlinear time series analysis. This approach leverages symplectic geometry to overcome the limitations of existing methods. Current techniques, including the correlation theorem, singular value decomposition (SVD), and false nearest neighbors [16], and Akaike information criterion [17], face challenges such as being data-intensive, subjective, time-consuming, and sensitive to noise and data length. In contrast, the proposed method considers factors like data length, sampling interval, and noise, yielding robust results.

2- 3- Granger Causality Index

As described in the previous section, Granger causality (GC), introduced by Wiener, offers a bivariate linear measure of causality. In this framework, if incorporating past values of Y improves the prediction of X, we conclude a causal connectivity from Y to X. The assessment of causality is determined using the following formula:

The previous p samples of X(t) and Y(t) are included in the AR model to forecast X:

$$X(t) = \sum_{j=1}^{P} [a(j)X(t-j) + b(j)Y(t-j)] + \varepsilon(t) \tag{1}$$

ε indicates the prediction error. Then X(t) is predicted by own past p samples:

$$X(t) = \sum_{j=1}^{P} c(j)X(t-j) + \varepsilon'(t) \tag{2}$$

ε' is the prediction error of X(t).

The index of linear Granger causality is defined below.

$$LGC_{Y \to X} = \ln \frac{\varepsilon'(t)^2}{\varepsilon(t)^2} \tag{3}$$

The conclusion of causality from y to x can be made if $LGC_{Y \to X}$ is significantly positive. However, this measurement is bivariate and cannot differentiate between direct and indirect connectivity. To address this limitation, a multivariate version based on the multivariate autoregressive (MVAR) model has been proposed in [18]. While this approach resolves the bivariate issue, it remains linear and may oversimplify nonlinear dynamic systems, leading to suboptimal results. In the following section, we will combine these methods to develop a proposed algorithm for measuring nonlinear conditional effective connectivity.

2- 4- Adaptive Neuro-Fuzzy Inference System Granger Causality (ANFISGC)

We explore a more advanced version of the MVAR model called ANFIS, which can effectively approximate both linear and nonlinear connectivity. In our analysis, we consider a system with N channels represented by $X_{n(t)}$, where n ranges from 1 to N and t ranges from 1 to L. To partition the data, we create two sets: X_n^{train}, which includes 75% of the X_n data, and X_n^{test}, which contains the remaining 25%. In this section, we focus on estimating the effective connectivity from X_β to X_α conditioned by X_γ ($\beta \to \alpha | \gamma$).

To extract the model order p using symplectic geometry, training sets of X_α, X_β, and X_γ are utilized. These three signals serve as inputs for ANFIS, with p-lagged samples of X fed into the system for prediction. To avoid overfitting during training, the error of test data is monitored over iterations, and training is stopped when the error curve starts to increase. To determine the optimal number of rules in ANFIS, the network is trained with different numbers of rules ranging from 3 to 50. The mean squared error (MSE) on the testing part of X_α is evaluated for each number of rules, and the number of rules that results in the lowest MSE is chosen as the best option.

$$\begin{aligned}\hat{x}_{\alpha\_model1}^{train}(t) = & f(x_\alpha^{train}(t-1), x_\alpha^{train}(t-2), \\ & ...,x_\alpha^{train}(t-p), \\ & x_\beta^{train}(t-1), x_\beta^{train}(t-2),...,x_\beta^{train}(t-p), \\ & x_\gamma^{train}(t-1), x_\gamma^{train}(t-2),...,x_\gamma^{train}(t-p))\end{aligned} \tag{4}$$

In 4, f is the learned ANFIS function with the least MSE obtained by training data, and $\hat{X}_{\alpha\_model1}^{train}$ is the prediction of $X_\alpha^{train}(t)$. The MSE is:

$$MSE_{\alpha\_model1}^{train} = \frac{1}{L\_training} \times \sum_{t=1}^{L\_training}(X_\alpha^{train}(t) - \hat{X}_{\alpha\_model1}^{train}(t))^2 \tag{5}$$

L_training is the length of the data.

Concerning Granger causality, the prediction precision is evaluated by examining the impact of lagged samples of Y. This evaluation leads to the conclusion that there exists a conditional causality link ($\beta \rightarrow \alpha | \gamma$). Now, the prediction of $X_\alpha^{train}(t)$ follows a similar method as described above, but the effect of delayed samples of X_β is not taken into consideration.

$$\hat{x}_{\alpha\_model2}^{train}(t) = g(x_\alpha^{train}(t-1), x_\alpha^{train}(t-2),$$
$$..., x_\alpha^{train}(t-p), x_\gamma^{train}(t-1), x_\gamma^{train}(t-2),$$
$$..., x_\gamma^{train}(t-p)) \tag{6}$$

$\hat{x}_{\alpha\_model2}^{train}(t)$ is the prediction value of $x_\alpha^{train}(t)$ without using $x_\beta^{train}(t)$ and g is the approximator function trained by ANFIS. MSE of this approximation is as follows:

$$MSE_{\alpha\_model2}^{train} = \frac{1}{L\_training}$$
$$\times \sum_{t=1}^{L\_training} (X_\alpha^{train}(t) - \hat{X}_{\alpha\_model2}^{train}(t))^2 \tag{7}$$

We define the measure of conditional effective connectivity or ANFISGC:

$$ANFISGC_{\beta \rightarrow \alpha | \gamma} = \ln \frac{MSE_{\alpha\_model2}^{train}}{MSE_{\alpha\_model1}^{train}} \tag{8}$$

An effective connectivity from X_β to X_α given X_γ is detected if d is significantly positive.

2- 5- Mutual Information

Mutual information was first introduced in classical information theory by Shannon in 1948. It is considered a nonparametric measure that quantifies both linear and nonlinear dependencies between two variables. In other words, it indicates how much knowing one variable reduces the uncertainty of another variable [19]. The mutual information between X and Y is defined by the following equation:

$$M_{XY} = \sum p(x,y) \log \frac{p(x,y)}{p(x)p(y)} \tag{9}$$

Various methods have been proposed to investigate information flow and measure causal interactions. For example, Hinrichs et al. utilized directed information flow (DIF) to assess causality in event-related experiments involving fMRI, EEG, and MEG [20]. Similarly, Seung-Hyun Jin et al. employed time-delayed mutual information (TDMI) to explore the contributions of nonlinear information flow in corticomuscular (CM) interactions [13]. While these studies successfully determine the direction of information flow, they do not clarify whether the connectivity is linear or nonlinear. This limitation arises because most existing methods measure both linear and nonlinear dependencies simultaneously, failing to differentiate between the various types of connectivity.

ANFISGC can extract effective connectivity but does not differentiate between linear and nonlinear connections; it simply categorizes connectivity as either present or absent. While mutual information can assess connectivity without considering direction, time-delayed mutual information (TDMI) does take direction into account [13]. In this research, we focus on using mutual information to characterize the type of connectivity, specifically to determine whether it is linear or nonlinear.

2- 6- Surrogate Test

Surrogate data is generated by manipulating the original data to create additional datasets for statistical analysis. This process preserves specific properties of the original data while introducing randomness in other aspects. There are several methods for generating surrogate data, and in this section, we specifically employed the Fourier-transformed surrogates' method. This approach helps identify the nature of the relationship between two signals.

To generate surrogate data, the following steps are taken. First, a Fourier transform is applied to the original data to obtain the complex amplitudes for each frequency. Next, these complex amplitudes are modified by randomizing their phases, which is done by adding a uniformly distributed random phase variable ϕ within the range $[0,2\pi)$ for each frequency. This randomization involves multiplying each complex amplitude by the complex exponential eiϕ. Finally, the modified spectrum is transformed back to the time domain to create the surrogate data. Importantly, the surrogate data retains the same mean, variance, and power spectrum as the original time series. In the bivariate surrogate data test, the phase randomization process is applied simultaneously to both the x and y time series, preserving all linear autocorrelations and cross-correlations between them [21]. The purpose of the bivariate surrogate test is to assess the relationship between the two signals and determine whether it can be represented by a linear model. Specifically, we evaluate whether there is connectivity between the x and y data through ANFISGC, and if so, whether this connectivity arises from nonlinear dependence, using the bivariate surrogate test. The flowchart in Figure 1 illustrates the overall procedure of the proposed method. The null hypothesis corresponds to the linear dependence of the two signals. If the null hypothesis is rejected, we can conclude that the time series has nonlinear dependence rather than a linear one.

To determine acceptance or rejection of the test, the significance level S is defined by:

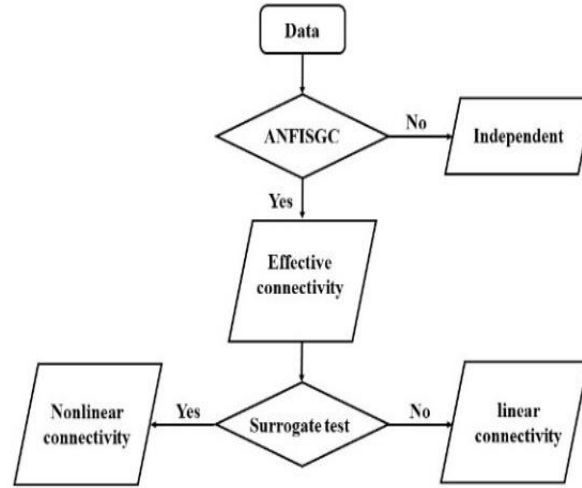$$S = \frac{|<MI_{surro}> - MI|}{\sigma(MI_{surro})} \tag{10}$$

Fig. 1. The proposed procedure diagram illustrates the steps involved in analyzing the connectivity between two time series. The first step is to use ANFISGC to extract connections, followed by the surrogate test to determine the type of connections. If the ANFISGC test results in rejection, it indicates that both time series are independent. In such cases, we can conclude that there is no significant connectivity between them. However, if the test does not result in rejection, it suggests that the total connectivity includes both linear and nonlinear connections. The next step is to perform the surrogate test. If this test is rejected, it indicates that the original two time series can be better represented by a nonlinear model, indicating the presence of nonlinear connectivity. On the other hand, if the surrogate test is not rejected, it implies that the total connectivity, which passed the ANFISGC test, primarily results from their linear connectivity. Overall, this procedure ensures a comprehensive analysis of the connectivity between two time series, helping to identify the nature of the connections and establish the appropriate model for representation.

$<MI_{surro}>$ and $\sigma(MI_{surro})$ respectively denote the mean value MI of surrogate data and standard deviation.

The hypothesis was rejected at a 0.95 level of significance if the value of S exceeded 1.65 [22]. To validate the methods outlined above, we generated simulated data and one hundred surrogate datasets for the hypothesis. The results section includes images that support the study's findings. We have carefully reviewed the research methodology and the formulas used, and we have clarified the assumptions regarding the conditional relationship between the two signals. In the following section, we describe the experimental data and the preprocessing steps undertaken to implement the proposed method.

2- 7- MEG and EEG data

To achieve the objectives of this research, we implemented our method on MEG, EEG, and multimodal data (MEEG). MEG and EEG signals were collected from ten epilepsy patients at Henry Ford Hospital in Detroit (HFH), MI, USA, and the data acquisition was approved by the HFH Institutional Review Board (IRB) committee [23]. The MEG signals were recorded using a 148-channel whole-head neuromagnetometer, while the EEG signals were captured with a 32-channel electrocap. Both MEG and EEG had a sampling frequency of 508 Hz. Data was collected from patients during the interictal period while they were at rest. Before applying the proposed method, we conducted

a series of preprocessing steps on the acquired data. First, we applied a band-pass filter with a frequency range of 3 to 50 Hz. To identify the epileptic zone, we transformed the surface-level data into brain source data using the Multiple Sparse Prior (MSP) technique to solve the inverse problem [24]. This process enabled us to reconstruct the time series of brain sources. We utilized the patients' structural MRI (sMRI) images to define the head meshes and address the forward problem. For the MEG data, we employed a single-shell model, while for the EEG data, we used the EEG BEM model. These models effectively captured the structural characteristics of the brain and facilitated the formulation of the forward problem. We then computed the gain matrix to represent 8,196 brain dipoles. All steps were simulated using the SPM Toolbox within MATLAB 2018, which provided a comprehensive suite of tools for brain imaging analysis and allowed for efficient computation of the lead field (gain) matrix. Figure 2 presents the reconstructed brain dipole sources, illustrating the spatial locations and strengths of brain activity identified through the inverse problem analysis. Figure 3 illustrates the formulation of the forward model.

After calculating the power of all 8,196 brain dipoles, we identified and retained those with power exceeding 30% of the maximum power. These selected dipoles, deemed dominant, correspond to regions of the brain exhibiting significant neural activity. To determine the anatomical regions associated with these dominant dipoles, we utilized
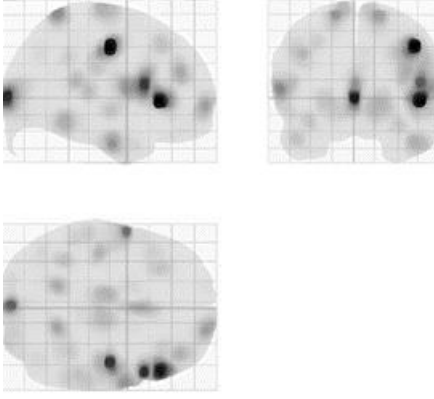
Fig. 2. Map of the power of the brain time series reconstructed from the MEG inverse problem.
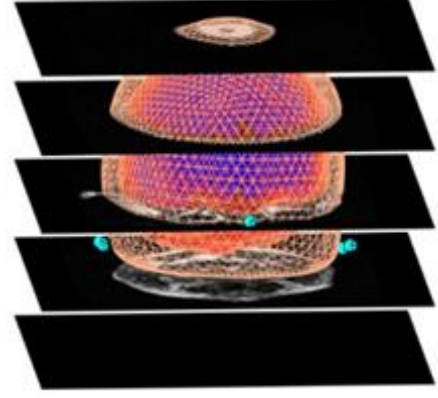

Fig. 3. This standard (Imaging) model in SPM defines the forward problem by mapping the activity of brain sources to the measured data. It incorporates the geometry and electrical properties of the head, as well as the distribution of the brain dipoles. The figure shows the canonical cortical mesh (blue), inner skull surface (red) and scalp surface (light brown).

the AAL atlas for labeling. Subsequently, we extracted the unified time series for all dipoles within the same Region of Interest (ROI) using Principal Component Analysis (PCA). This technique allows us to reduce the dimensionality of the data while preserving the most significant temporal variations among the selected dipoles within each ROI.

However, due to the ill-posed nature of the inverse problem, we encountered zero-phase correlations among the signals obtained from PCA. To mitigate this issue, we applied a leakage correction method [25].

Finally, we applied the ANFISGC connectivity measure to the corrected time series.

3- Results

To ensure the robustness and validity of the proposed ANFISGC (Adaptive Neuro-Fuzzy Inference System Granger Causality) approach in detecting effective connectivity, a set of controlled simulations was designed. Specifically, three synthetic time series were generated, each consisting of 4000 samples. These signals incorporated white Gaussian noise terms (ε1, ε2, and ε3), with variances matched to those of the original signals to simulate realistic noise levels. The signal-to-noise ratio (SNR) was fixed at 0 dB to create a challenging scenario for causality detection, mirroring real-world neural recordings where noise is often significant [11]. The simulated time series were constructed to embed both nonlinear dynamics and inter-signal causal dependencies. The mathematical formulations of the signals are as follows:

$$
\begin{aligned}
x_1(n) &= 3.4x_1(n-1)(1-x_1^2(n-1))e^{-x_1^2(n-1)} + \varepsilon_1(n) \\
x_2(n) &= 3.4x_2(n-1)(1-x_2^2(n-1))e^{-x_2^2(n-1)} \\
&\quad + 0.5x_2(n-1)x_1(n-1) + \varepsilon_2(n) \\
x_3(n) &= 3.4x_2(n-1)(1-x_2^2(n-1))e^{-x_2^2(n-1)} \\
&\quad + 0.3x_2(n-1) + 0.5x_1^2(n-1) + \varepsilon_3(n)
\end{aligned}
\tag{11}
$$

These equations define a coupled system where each signal exhibits both self-dynamics and cross-dependencies. The signal $x_1(n)$ evolves independently with complex nonlinear behavior, while $x_2(n)$ depends both on its previous value and that of $x_1(n)$, thus introducing a directed causal link $x_1 \rightarrow x_2$. Similarly, $x_3(n)$ is influenced by both x_1 and x_2, reflecting the causal paths $x_1 \rightarrow x_3$ and $x_2 \rightarrow x_3$. This example serves as an effective simulation model for investigating the capabilities of ANFISGC in detecting both linear and nonlinear connectivity in effective connectivity. Since the ground truth structure of the interdependencies is known, the performance of ANFISGC can be quantitatively assessed. To establish causality, the following two principles must be upheld:

1. The causality value of β→α|γ should be positive. A negative value suggests that the β signal does not contribute to the prediction of the α signal.

2. The causality value of β→α|γ must be greater than the (1-p_value) multiplied by 100 percentile of the null distribution.

Figure 4 illustrates the histogram of the resulting ANFISGC for 100 surrogate data (depicted in blue). To fulfill the conditions above, if the (1-p)×100 percentile of the null distribution is positive, it is considered the threshold (shown as the green line).
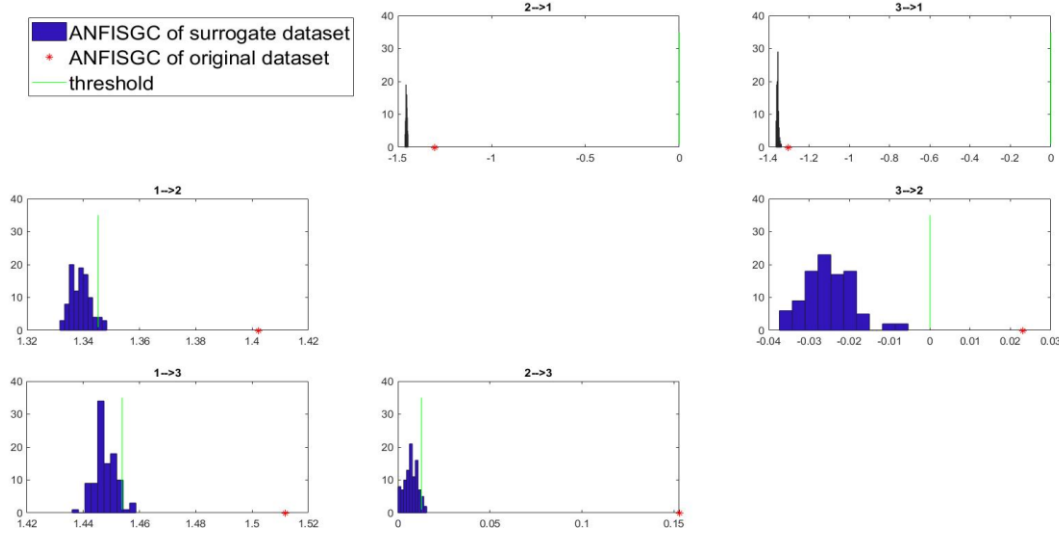
Fig. 4. Histograms of the ANFISGC values for both original and surrogate data are used to investigate connectivity in the simulation data. ANFISGC accurately captures connectivity based on the Granger Causality index, particularly concerning the right side's threshold.

If not, the threshold is set to zero. The causal coupling $(\beta \rightarrow \alpha | \gamma)$ is only confirmed if the of the original data (represented by a red star in Figure 4) exceeds the threshold. As you can see in Table 1, ANFISGC accurately identifies and effectively connects.

To evaluate the performance of the surrogate test based on Mutual Information (MI) for the second phase of the research, we generated two sets of simulated data representing linear and nonlinear relationships:

$$y(n) = x(n-1) + 10x(n-1)^3 + \varepsilon(n)$$
$$y(n) = 10x(n-1) + \varepsilon(n) \quad (12)$$

x is a random signal with a length of 50 data points, and ε is a white Gaussian noise. The MI between two signals, x and y, obtained from both linear and nonlinear equations, is calculated. We obtained results for 200 pairs of signals, x and y. Their mutual information (MI) histogram is represented in Figure 5, multiplied by 100 percentiles of the null distribution. As in Figure 5, it is clear that the number of signals that have a linear relationship with the group of signals that have a nonlinear relationship are completely separated in such a way that they form two null and alternative hypotheses.

From another perspective, as discussed in the previous section, normalizing the Fourier transform phases of the signals x and y individually generates what is known as "surrogate data." This data removes any nonlinear relationships while preserving linear associations. To validate this approach, we again compute The results are shown in Figures 6 and 7, which display data for 200 pairs of signals—half exhibiting linear relationships and the other half nonlinear relationships. It is clear that, for linear relationships, the mutual information

Table 1. The connectivity results of ANFISGC for simulation data.

To	From		
	X1	X2	X3
X1	0	0	0
X2	1	0	0
X3	1	1	0

(MI) for the original and surrogate data falls within a similar range. In contrast, for nonlinear relationships, the MI of the original data does not align with that of the surrogate data. the mutual information (MI) for both the original signal pairs and their surrogate data.

This outcome is expected because nonlinear relationships are not preserved in the surrogate data, leading to a significant difference in their mutual information (MI) values. These findings highlight the effectiveness of the normalization procedure, particularly in distinguishing between linear and nonlinear relationships. To further investigate the performance of MI, we calculate it for various values of "c" and "p," resulting in Tables 2 and 3.

$$y(n) = x(n-1) + cx(n-1)^p + \varepsilon(n) \quad (13)$$

Based on the information in Table 2, it seems that the accuracy of relationship-type assessments using surrogate
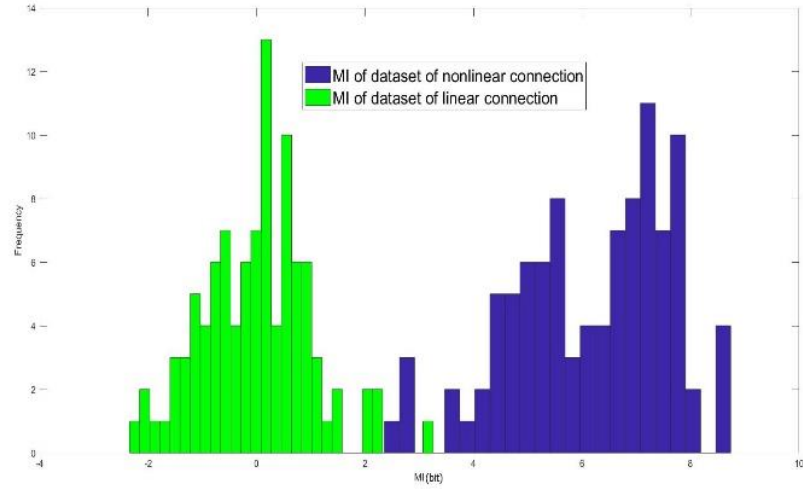
Fig. 5. Distribution of mutual information (MI) for 200 pairs of linear and nonlinear signal relationships. The difference in the range of MI values corresponding to linear and nonlinear relationships helps us identify the type of relationship between real signals.
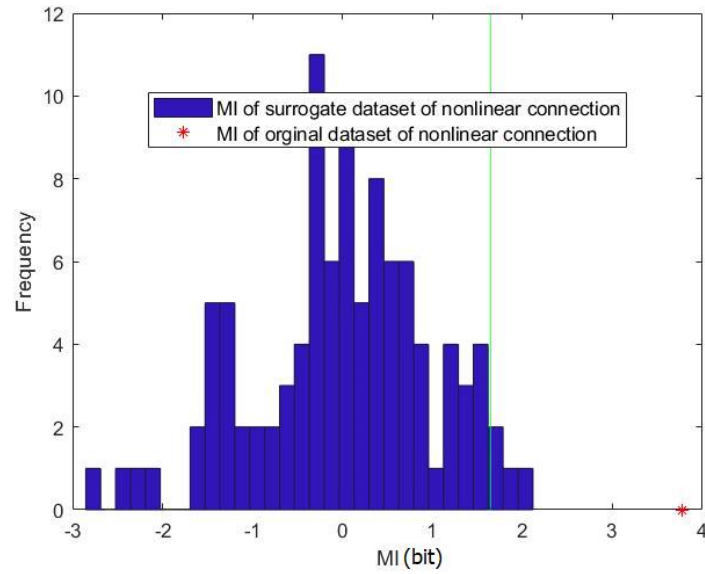

Fig. 6. MI related to the real signals x and y, as well as their surrogate data, is presented here. The red star and blue histogram represent the MI value associated with the nonlinear relationship between x and y and their surrogate data. The difference in the MI value ranges between the real signals x, y and the associated surrogate data, as shown in Figure 5, indicates that the relationship between x and y is nonlinear(S>1.65).
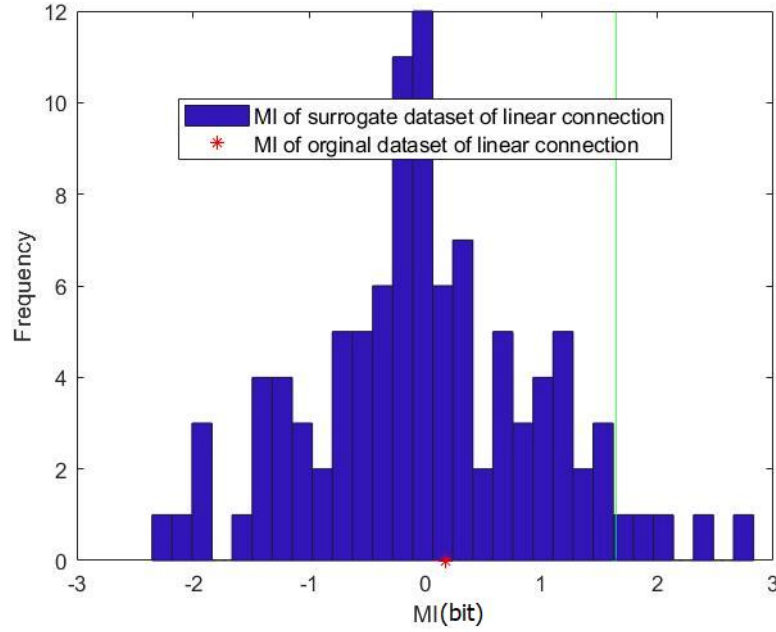
Fig. 7. The red star and blue histogram indicate the MI for the linear relationship between x and y and their surrogate data. Using a similar approach, due to the overlap in the range of MI values between the signals x, y, and the surrogate data, we conclude that the relationship between x and y is linear(S<1.65).

data-based mutual information is influenced by the gradient of the relationship. Specifically, as the degree of nonlinearity between the two signals increases (as indicated by the power term in Equation 13), the accuracy of predicting nonlinear relationships also rises, and vice versa. In other words, the ability to distinguish between linear and nonlinear relationships improves with the strength of the nonlinearity. This observation indicates that the method is effective in discerning the nature of the relationship between signals based on their mutual information. The presence of a significant nonlinear component seems to enhance the accuracy in determining whether the relationship is linear or nonlinear.

Next, let's apply these methods to recorded data from epilepsy patients.

To start, EEG, MEG, and MEEG data were collected from a single patient. Following the preprocessing steps outlined in Section II and solving the inverse problem, effective

Table 2. Assessment of relationship types using surrogate data-based mutual information for various values of "c" and "p".

Parameters	Nonlinearity prediction accuracy
c = 10, p = 2	68%
c = 10, p = 3	94%
c = 10, p = 4	100%
c = 10, p = 5	100%

relationships between brain regions of interest (ROIs) were established, as illustrated below. The region that exhibits the most effective connectivity with others is referred to as the dominant region (DR).

Table 3. The accuracy of nonlinearity measurement with different values of c and a fixed value of p (where p=3) using MI and surrogate data.

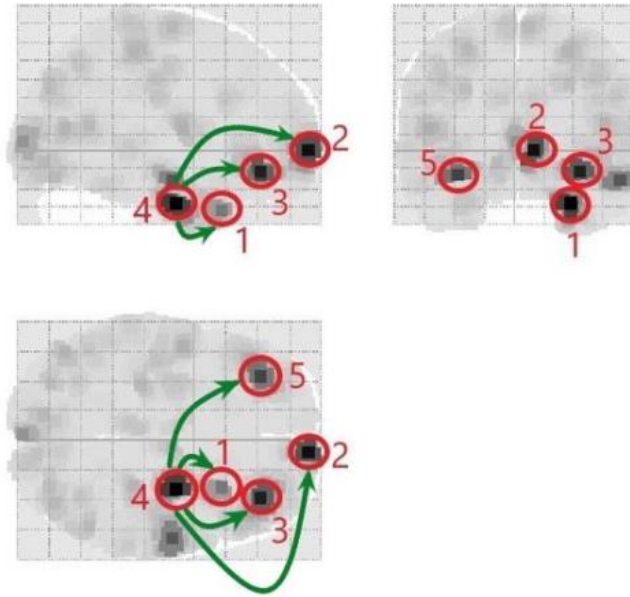| Parameters	c = 0.5, p =3	c = 1 , p = 3	c = 2 , p = 3	c = 4 , p = 3	c = 8 , p = 3
Nonlinearity prediction accuracy	34%	53%	76%	95%	97%

Fig. 8. The regions of interest (ROIs) related to the MEG data for patient EP0088 are illustrated, showing the power of signals from different areas of the brain across the sagittal, axial, and coronal planes. The ParaHippocampal_R region has been identified as the dominant area due to its most effective relationships with other ROIs, which include: 1. Fusiform_R, 2. Frontal_Med_Orb_R, 3. OFCant_R, 4. ParaHippocampal_R, and 5. OFCant_L.

Table 4. Results related to DRs for all epilepsy patients across the EEG, MEG, and MEEG datasets.

Patiens	MEG	EEG	MEEG	IE*
EP0088	ParaHippocampal_R	Calcarine_L / Precentral_R	Temporal_Pole_Mid_R	R
EP0180	Frontal_Sup_Medial_R / Olfactory_L	Temporal_Mid_L	Temporal_Inf_R	L
EP1041	Fusiform_L / Temporal_Inf_R / Temporal_Mid_R	OFClat_R	Temporal_Pole_Mid_L	R
EP1045	OFCant_R	Temporal_Pole_Mid_L	Angular_L / OFCant_R / Parietal_Sup_L	R
EP1158	Fusiform_L	Calcarine_L / SupraMarginal_L	Postcentral_L	R

* IE; Intracranial evaluation

The table indicates that the reported hemispheres for seizure foci exhibit similarities across different recording methods in some instances—suggesting consistency in localization—while in other cases, discrepancies are observed, which may be due to methodological differences, variability in seizure propagation, or limitations in the accuracy of certain techniques.

The subsequent table presents the assessment of the types of effective relationships for each reported dominant region (DR) in Table 4, along with the calculated significance level (S) values. As mentioned earlier, relationships are classified as linear when S is less than 1.65, and nonlinear otherwise. Additionally, Table 5 provides an example of connectivity between the DR area and other regions in some

Table 5. Values for the type of connectivity measurements between the dominant region (DR) and other brain regions for all patients.

Patient	Data	DR	*R1	R2	R3	R4	R5	R6
EP0088	MEG	ParaHippocampal_R	5.8	0.8	3.5	3.9		
	EEG	Calcarine_L	16.9	15.3				
		Precentral_R	17.3	23.4				
	MEEG	Temporal_Pole_Mid_R	5.5	6.3	5.8	5.3	10.8	
EP0180	MEG	Frontal_Sup_Medial_R	11.9	9.6	11	10.4	10.2	
		Olfactory_L	10.4	10.7	5.4	9.6	4.5	
	EEG	Temporal_Mid_L	0.9	3.2	1.4	1.8	0.8	
	MEEG	Temporal_Inf_R	6.7	5.6	4.7	2.7	1.9	
EP1041	MEG	Fusiform_L	1.8	2.2	0.7	2.1	3	3
		Temporal_Inf_R	1	0.7	0.1	0.2	0.6	1
		Temporal_Mid_R	1.9	0.6	1.9	0.1	2.3	1.9
	EEG	OFClat_R	0.2	0.3	2.5	2	2.3	2.2
	MEEG	Temporal_Pole_Mid_L	2.4	2.1	2.3	3.6	2.7	
EP1045	EEG	OFCant_R	0.4	1.8	1.8	1.7	1.7	
	MEG	Temporal_Pole_Mid_L	0.3	0.5	3.6	0.1	1.4	2.3
	MEEG	Angular_L	2	2.4	2.1	3.2	1.4	2.6
		OFCant_R	2	0.1	2.1	2.7	1.3	2.4
		Parietal_Sup_L	2.5	2	2.4	2.4	2.7	1.4
EP1158	EEG	Fusiform_L	3.5	2.8	2.7	2.8	1.9	
	MEG	Calcarine_L	0	1.5	1.7	0.3		
	MEEG	SupraMarginal_L	1.8	1	1.1	0.9		
		Postcentral_L	5.2	6.3	4.5	6.8		

patients. In this case, we focus on patient EP1045, where the significance levels of S for all patients are shown. The types of effective relationships between the DR and other areas related to MEG exhibit varying S values, such as 1.78 and 1.68, among others.

4- Discussion

The dominant areas for all the patients in the case of EEG, MEG, and MEEG datasets were obtained. The results demonstrated that the reported DRs were not necessarily located in the common hemisphere of the brain. This suggests that using both EEG and MEG datasets simultaneously will not be efficient in detecting the dominant spots for epilepsy. For instance, in patient EP0088, the DRs identified from EEG, MEG, and MEEG were Precentral_R, ParaHippocampal_R, and Temporal_Pole_Mid_R, respectively—all located in the right hemisphere. In contrast, patient EP0180 exhibited DRs in Temporal_Mid_L, Olfactory_L, and Temporal_Inf_R for EEG, MEG, and MEEG, respectively, indicating a lack of hemispheric consistency. These results, detailed in Table 4, highlight the complexity and variability of DR localization across different modalities.

On the other hand, based on the values presented in Tables 2 and 3, it can be inferred that a relationship characterized by an S-value less than 1.65 is not necessarily purely linear. The S-index is sensitive to the gradient of the nonlinear component (power p), which influences the nonlinearity in the relationship between two signals. Therefore, even relationships classified as linear by this threshold may contain a non-negligible nonlinear contribution. Taken together, these findings suggest that the simultaneous analysis of EEG and MEG data does not inherently improve the reliability of DR detection.

In a study in 2018, DR values were measured using only

MEG data with the ANFISGC method in epileptic patients. In contrast with our study, only one DR was reported for each patient [6]. Another difference with this study is that, in addition to determining cause and effect relationships between brain regions, we have determined the type of these relationships, which means which ones are linear and which ones are nonlinear. The measurement of the type of communication has also been done in research in 2019, in which the amount of participation of the linear and non-linear parts in an effective relationship has been calculated in a specific way, and the intensity of each is determined [11].

During research in the same year, the coefficient of participation of the linear part in an effective non-linear relationship was calculated, which provides information from both the linear and non-linear parts in the same relationship. The measurement of the type of relationship in our study was done in a binary way, which means that we assumed the relationship is either linear or non-linear. A weakness of our method is that the degrees of participation of the linear and non-linear parts are not calculated. There is no information about the effective relationship. For example, in Table 5, the significance level of S is shown for all patients. We consider patient EP1045 as an example. The type of effective relationships between DR and other areas related to MEG has adopted variable S with values of 1.78, 1.68, etc. According to our default, all these relationships are considered non-linear due to the large S value of 1.65, but on the other hand, these values are not much different from the threshold limit of 1.65, and this is indicative of the fact that the linear part can be involved in these effective relationships. In the next step of the study, the surrogate data results based on mutual information were implemented on the simulated data with different coefficients (intensity) and powers, and we obtained different accuracies of intensity (coefficient c). In these cases, it is better to express the result in this way that the intensity of the non-linear part, both in terms of the gradient and the coefficient, is much less, to the point where it may be completely zero, and only the linear part is involved in the effective relationship. However, due to the binary nature of the test, we do not know it.

5- Conclusion

The study examined dominant areas in patients using EEG, MEG, and MEEG datasets to identify regions associated with epilepsy. Results indicated that these dominant regions (DRs) were not always in the same hemisphere, suggesting that using EEG and MEG data together may not enhance the detection of epileptic areas. For instance, patient EP0088 showed DRs in the right hemisphere, while EP0180 had areas across both hemispheres, complicating the diagnosis.

The research also identified both linear and nonlinear relationships. However, it pointed out that the binary classification (linear or nonlinear) used in this analysis did not capture the degree of involvement of each relationship type. Further testing showed that even relationships deemed linear might still contain significant nonlinear components, emphasizing the limitations of the current analytical approach.

6- Future Work

To more comprehensively measure the type of effective relationships in the study of the brain network of epilepsy patients, we can obtain a relationship that maps the input signals to the output signal for prediction, and by using methods such as z-transformation and Taylor expansion, we can determine the linear and non-linear parts of this input-output relationship. In this way, in addition to the participation rate of each compartment, we can have a comparison with what the mutual information method obtains. The reports obtained for the DR of epileptic patients completely depend on the interictal interval or IED, which is detected during the time series of the EEG signal by an epileptologist. It is necessary to perform this operation accurately to obtain the correct results for the dominant brain regions of the patients. In determining the type of effective relationships, it is possible to create histograms for each of the identified effective relationships by using mutual information and surrogate data techniques, such as measuring the validity of effective relationships, to conduct a more comprehensive study of the brain networks of epilepsy patients.

References

[1] J. Liu, Li, M., Pan, Y., Lan, W., Zheng, R., Wu, F. X., & Wang, J., Complex Brain Network Analysis and Its Applications to Brain Disorders: A Survey, Complexity, 8362741 (2017).

[2] M. Ding, Chen, Y., & Bressler, S. L., Granger causality: basic theory and application to neuroscience, Handbook of time series analysis: recent theoretical developments and applications, (2006) 437–460.

[3] C. Mahjoub, Bellanger, J. J., Kachouri, A., & Le Bouquin Jeannes, R., On the performance of temporal Granger causality measurements on time series: a comparative study, Signal, Image and Video Processing, 14 (2020) 955–963.

[4] N. Talebi, Nasrabadi, A. M., Mohammad-Rezazadeh, I., & Coben, R., NCREANN: Nonlinear causal relationship estimation by artificial neural network; applied for autism connectivity study, IEEE transactions on medical imaging, 38 (2019) 2883–2890.

[5] Z. Abbasvandi, & Nasrabadi, A. M., A self-organized recurrent neural network for estimating the effective connectivity and its application to EEG data, Computers in biology and medicine, 110 (2019) 93–107.

[6] D.M. Khan, Yahya, N., Kamel, N., & Faye, I., Automated diagnosis of major depressive disorder using brain effective connectivity and 3D convolutional neural network, IEEE Access, 9 (2021) 8835–8846.

[7] A. Saeedi, Saeedi, M. Maghsoudi, A., & Shalbaf, A., Major depressive disorder diagnosis based on effective connectivity in EEG signals: A convolutional neural network and long short-term memory approach, Cognitive neurodynamics, 15 (2021) 239–252.

[8] R. Das, Sen, S., & Maulik, U., A survey on fuzzy deep neural networks, ACM Computing Surveys (CSUR), 53

(2020) 1–25.

[9] M. Rahimi, Davoodi, R., & Moradi, M. H., Deep fuzzy model for non-linear effective connectivity estimation in the intuition of consciousness correlates, Biomedical Signal Processing and Control, 57 (2020) 101732.

[10] N. Jamali, Sadegheih, A., Lotfi, M. M., Wood, L. C., & Ebadi, M. J., Estimating the depth of anesthesia during the induction by a novel adaptive neuro-fuzzy inference system: a case study, Neural Processing Letters, 53 (2021) 131–175.

[11] M. Farokhzadi, Hossein-Zadeh, G. A., & Soltanian-Zadeh, H., Nonlinear effective connectivity measure based on adaptive neuro fuzzy inference system and Granger causality, NeuroImage, 181 (2018) 382–394.

[12] B. Samanta, Prediction of chaotic time series using computational intelligence. Expert Systems with Applications, 38 (2011) 11406–11411.

[13] S.H. Jin, Lin, P., & Hallett, M., Linear and nonlinear information flow based on time-delayed mutual information method and its application to corticomuscular interaction, Clinical Neurophysiology, 121 (2010) 392–401.

[14] N. Walia, Kumar, S., & Singh, H., A survey on applications of adaptive neuro fuzzy inference system, International Journal of Hybrid Information Technology, 8 (2015) 343–350.

[15] Y. Liu, & Aviyente, S., Quantification of effective connectivity in the brain using a measure of directed information, Computational and mathematical methods in medicine, 2012 (2012) 635103.

[16] M. Lei, Wang, Z., & Feng, Z., A method of embedding dimension estimation based on symplectic geometry, Physics Letters A, 303 (2002) 179–189.

[17] H. Akaike, Information theory and an extension of the maximum likelihood principle, In Selected papers of Hirotugu Akaike, (1998) 199–213.

[18] A. Khadem, & Hossein-Zadeh, G. A., Estimation of direct nonlinear effective connectivity using information theory and multilayer perceptron, Journal of Neuroscience Methods, 229 (2014) 53–67.

[19] J. Walters-Williams, & Li, Y., Estimation of mutual information: A survey, In International Conference on Rough Sets and Knowledge Technology, (2009) 389–396.

[20] H. Hinrichs, Noesselt, T., & Heinze, H. J., Directed information flow—A model-free measure to analyze causal interactions in event-related EEG-MEG-experiments, Human brain mapping, 29 (2008) 93–206.

[21] D. Prichard, & Theiler, J., Generating surrogate data for time series with several simultaneously measured variables, Physical Review Letters, 73 (1994) 951.

[22] M.N. Islam, & Islam, N., Retrospective study of 273 deaths due to poisoning at Sir Salimullah Medical College from 1988 to 1997, Legal medicine, 5 (2003) S129–S131.

[23] K. Jafari-Khouzani, Elisevich, K. V., Patel, S., & Soltanian-Zadeh, H., Dataset of magnetic resonance images of nonepileptic subjects and temporal lobe epilepsy patients for validation of hippocampal segmentation techniques, Neuroinformatics, 9 (2011) 335–346.

[24] J.D. López, Litvak, V., Espinosa, J. J., Friston, K., & Barnes, G. R, Algorithmic procedures for Bayesian MEG/EEG source reconstruction in SPM NeuroImage, 84 (2014) 476–487.

[25] G.L. Colclough, Brookes, M. J., Smith, S. M., & Woolrich, M. W., A symmetric multivariate leakage correction for MEG connectomes, Neuroimage, 117 (2015) 439–448.